Eur. Phys. J. C 47, 45–55 (2006)
Digital Object Identifier (DOI) 10.1140/epjc/s2006-02562-2

THE EUROPEAN PHYSICAL JOURNAL C

Reconciling ϕ radiative decays with other data for $a_0(980)$, $f_0(980)$, $\pi\pi \to KK$ and $\pi\pi \to \eta\eta$

D.V. Bugg[a]

Queen Mary, University of London, London E14NS, UK

Received: 10 March 2006 /
Published online: 19 May 2006 –

Abstract. Data for $\phi \to \gamma(\eta\pi^0)$ are analysed using the KK loop model and compared with parameters of $a_0(980)$ derived from Crystal Barrel data. The $\eta\pi$ mass spectrum agrees closely and the absolute normalisation lies just within errors. However, BES parameters for $f_0(980)$ predict a normalisation for $\phi \to \gamma(\pi^0\pi^0)$ at least a factor 2 lower than is observed. This discrepancy may be eliminated by including constructive interference between $f_0(980)$ and σ. The magnitude required for $\sigma \to KK$ is consistent with data on $\pi\pi \to KK$. A dispersion relation analysis by Büttiker, Descotes-Genon and Moussallam of $\pi\pi \to KK$ leads to a similar conclusion. Data on $\pi\pi \to \eta\eta$ also require decays of σ to $\eta\eta$. Four sets of $\pi\pi \to KK$ data all require a small but definite $f_0(1370)$ signal.

PACS. 13.25.Gv; 14.40.Gx; 13.40.Hq

1 Introduction

Data for $\phi(1020) \to \gamma(\eta\pi^0)$ and $\gamma(\pi^0\pi^0)$ from Novosibirsk [1–3] and the KLOE collaboration at Daphne [4, 5] may throw light on $a_0(980)$ and $f_0(980)$, as Achasov and Ivanchenko pointed out in 1989 [6]. A vigorous debate has followed the publication of data. An extensive list of references is given in a recent paper of Boglione and Pennington [7].

Figure 1 shows the model conventionally assumed for radiative ϕ decays. Both the $\phi \to K^+K^-$ decay and rescattering at the f_0 (or a_0) vertex are short-ranged. In the intermediate state, kaons propagate to larger radii where they radiate a photon through an electric dipole moment.

These data provide information only on the lower sides of $a_0(980)$ and $f_0(980)$, i.e. their coupling to $\eta\pi$ and $\pi\pi$. There is no direct information on their coupling to KK, except by assuming the KK loop model and using the absolute normalisation. For $\gamma(\eta\pi^0)$, this normalisation depends on the product $g^2[a_0(980) \to \eta\pi] \times g^2[a_0(980) \to KK]$. In order to test the model, a comparison is made with parameters of $a_0(980)$ from high statistics Crystal Barrel data on $\bar{p}p \to \pi^0(\eta\pi^0)$ [8] and $\bar{p}p \to \omega(\eta\pi^0)$ [9]. There is agreement within the errors, supporting the KK loop model.

The BES collaboration has made an accurate determination of $f_0(980)$ parameters from $J/\Psi \to \phi\pi^+\pi^-$ and ϕK^+K^- data [10]. Their values of g^2 predict a normalisation for $\phi \to \gamma(\pi^0\pi^0)$ a factor 2 smaller than observed in both Novosibirsk and Daphne data, if $f_0(980)$ alone is responsible. This discrepancy is resolved by adding a broad component coupling to both $\pi\pi$ and KK and interfering constructively with $f_0(980)$. It may be parametrised as the high mass tail of the σ pole, although other interpretations are possible, e.g. those of Au, Morgan and Pennington [11] and of Anisovich, Anisovich and Sarantsev [12].

This broad component should also appear in $\pi\pi \to KK$. It will be shown that it can indeed be accomodated naturally there. A similar broad component is required to fit data on $\pi\pi \to \eta\eta$. A combined fit is made to data on $\pi\pi$ elastic scattering, $\pi\pi \to KK$ and $\pi\pi \to \eta\eta$. The $\pi\pi$ phase shifts and elasticities are taken from the re-analysis by Bugg, Sarantsev and Zou [13] of moments from Cern–Munich data [14].

Formulae are discussed in Sect. 2. Readers interested only in results can skip this formalism. An awkward problem arises in parametrising $\pi\pi \to KK$ near 1 GeV. The broad component and $f_0(980)$ both go through 90° at ~ 1 GeV. It is difficult to find a parametrisation which accomodates both resonances while still satisfying unitarity. The scheme which is adopted here is driven by the features of the data and is explained in Sect. 2.

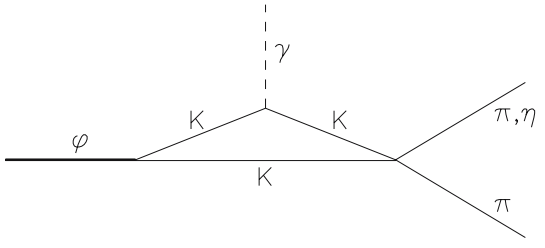

Fig. 1. The KK loop model for ϕ radiative decays

[a] e-mail: D.Bugg@rl.ac.uk

Sects. 3 and 4 then report the fits to data on $\phi \to \gamma(\eta\pi^0)$ and $\gamma(\pi^0\pi^0)$. Section 5 concerns the fit to $\pi\pi \to KK$ and $\eta\eta$, using parameters consistent with $\phi \to \gamma(\pi^0\pi^0)$. A brief summary is given in Sect. 6.

2 Formulae

2.1 ϕ radiative decays

Close, Isgur and Kumano [15] give formulae for the mass distribution of $\pi\pi$ or $\pi\eta$ pairs predicted by the KK loop model. It is important to keep track of the absolute normalisation and also write formulae in a way where the comparison between $\pi^0\pi^0$ and $\pi\eta$ is as simple as possible. With some trivial re-arrangement of symbols, their equations (3.6) and (3.7) may be written for $\phi \to \gamma(\pi^0\pi^0)$ as:

$$\frac{\mathrm{d}\Gamma}{\mathrm{d}m} = |I(a,b)|^2 \frac{\alpha g_\phi^2 g^2_{K^+K^-} g^2_{\pi^0\pi^0}}{|D(s)|^2}\chi \quad (1)$$

$$\chi = \frac{m_{\pi\pi} k_\gamma^3 \rho_{\pi\pi}(s)}{96\pi^6 m_K^4} \quad (2)$$

$$k_\gamma = \frac{m_\phi^2 - s}{2m_\phi} . \quad (3)$$

Here s is the invariant mass squared of the $\pi\pi$ pair, k_γ is the photon momentum, m are masses, α is the fine-structure constant $\simeq 1/137$ and $I(a,b)$ is a formula for the KK loop integral given by equations (3.4) and (3.5) of Close et al; the quantities a and b are defined there. The cubic dependence on k_γ arises from gauge invariance and is the familiar E_γ^3 factor for an E1 transition. The denominator $D(s)$ in (1) is written for $f_0(980)$ in the Flatté form:

$$D(s) = M^2 - s - \frac{i}{16\pi}\left[g^2_{\pi\pi}\rho_{\pi\pi}(s) + g^2_{KK}\rho_{KK}(s)\right] ; \quad (4)$$

the factor $1/16\pi$ follows the definition used by the Particle Data Group [16] in their equation (38.17), after allowing for a factor 4π from integrating the S-wave over angles. Equation (4) is the form used by KLOE. Note that values of g^2 in this equation refer to the sum over charge states:

$$g^2_{\pi\pi} = 3g^2_{\pi^0\pi^0} = (3/2)g^2_{\pi^+\pi^-} \quad (5)$$

$$g^2_{KK} = 2g^2_{K^0K^0} = 2g^2_{K^+K^-} . \quad (6)$$

The BES collaboration writes the Flatté form using

$$g_1' \equiv \frac{g^2_{\pi\pi}}{16\pi} \quad (7)$$

$$g_2' \equiv \frac{g^2_{KK}}{16\pi} . \quad (8)$$

Below the KK threshold, $\rho_{KK}(s)$ in (4) needs to be continued analytically as $+i\sqrt{4m_K^2/s - 1}$.

Equation (3.1) of Close et al. defines g_ϕ^2 via:

$$\Gamma(\phi \to K^+K^-) = \frac{g_\phi^2}{48\pi m_\phi^2}\left(m_\phi^2 - 4m_K^2\right)^{3/2} . \quad (9)$$

The coupling constants g^2 for f_0 decay are defined to have dimensions of GeV^2, but g_ϕ^2 is dimensionless and so is $I(a,b)$. Dimensions of (1) and (2) balance between left and right-hand sides; this was not apparent in the papers of either Close et al. or Achasov and Ivanchenko, since they replace $g^2_{\pi\pi}g^2_{KK}$ by a single g^2. The two powers of g^2 appear explicitly in the KLOE publication [5]. The relative normalisation of data on $\phi \to \gamma(\pi^0\pi^0)$ and $\pi \to \gamma(\eta\pi^0)$ will play an important role:

$$\frac{(\mathrm{d}\Gamma/\mathrm{d}m)_{\pi^0\pi^0}}{(\mathrm{d}\Gamma/\mathrm{d}m)_{\eta\pi^0}} = \frac{g^2_{f_0KK}\left(g^2_{f_0\pi\pi}/3\right)|D(s)|^2_{a_o}\rho_{\pi\pi}(s)}{g^2_{a_0KK}g^2_{a_0\pi\eta}|D(s)|^2_{f_o}\rho_{\eta\pi}(s)} . \quad (10)$$

2.2 Identical particles

At this point, it is necessary to pause and ask whether decays to $\pi^0\pi^0$ are affected by the fact that they are identical particles, whereas $\pi^0\eta$ are not. This is a tricky point. An $I = 0$ f_0 couples to the isospin combination $(\pi^+\pi^- + \pi^-\pi^- - \pi^0\pi^0)/\sqrt{3}$, where the coefficients are isospin Clebsch-Gordan coefficients. Experimentally, the $\pi^+\pi^-$ integrated cross section may be obtained by counting π^+ over 4π solid angle. There are two amplitudes, one for producing a π^+ at angle θ, say, and the the other for producing a π^- at that angle and an accompanying π^+ at angle $(\theta + \pi)$. Both are in S-waves, so at angle θ there is a total amplitude for π^+ of $2/\sqrt{3}$. Integrating over 4π solid angle, the intensity of observed π^+ is $(4/3)4\pi$. For the $\pi^0\pi^0$ case, there are likewise two π^0 at angles θ and $(\theta + \pi)$ so the total π^0 amplitude is $2\pi^0/\sqrt{3}$. In this case, the integration should be only over 2π solid angle, so as to avoid counting π^0 pairs twice; the integrated intensity is $(4/3)2\pi$. The total $\pi\pi$ intensity is 8π, compared with the total $\eta\pi$ intensity of 4π, where there are no effects for identical particles.

So the $\pi\pi$ amplitude is increased by a factor 2 by the identity of the two pions. However, it is essential to remember that this factor 2 appears also in the Breit–Wigner denominator. The Breit–Wigner amplitude becomes

$$f = \frac{g_{K^+K^-}g_{\pi^0\pi^0}(2/\sqrt{2})(1/\sqrt{3})}{M^2 - s - i\left[2g^2_{\pi\pi}\rho_{\pi\pi} + g^2_{KK}\rho_{KK}\right]} . \quad (11)$$

In the numerator, the factor 2 allows for the doubling of the $\pi\pi$ amplitude by identity of the two pions and the factor $1/\sqrt{2}$ allows for the fact the π^0 are to be considered only over 2π solid angle. However, experimentalists do not write the Breit–Wigner amplitude in this way. They ignore identical particle effects and write it in all cases as

$$f = \frac{G_{K^+K^-}G_{\pi\pi}/\sqrt{3}}{M^2 - s - i\left[G^2_{\pi\pi}\rho_{\pi\pi} + G^2_{KK}\rho_{KK}\right]}, \quad (12)$$

where $G = g\sqrt{2}$. It is essential to remember this convention when using Breit–Wigner parameters deduced in the BES experiment. The upshot is that in comparing with Kloe data, one should use (12) and there is no effect from the identity of the pions in the final state.

2.3 How to treat the σ pole

In the KLOE analysis of $\phi \to \gamma(\pi^0\pi^0)$, a further contribution was included from the σ pole. This requires some discussion. For elastic $\pi\pi$ scattering, the amplitude may be written

$$f_{\rm el} = \frac{N(s)}{D(s)} \tag{13}$$

and there is a zero in $N(s)$ at the Adler point $s \sim 0.5m_\pi^2$, just below threshold [17]. The Adler zero is a basic feature of chiral perturbation theory and figures prominently in the series of papers on σ, κ, $f_0(980)$ and $a_0(980)$ by Oset and collaborators [18–23]. Data on $J/\Psi \to \omega\sigma$ may be fitted in both magnitude and phase using

$$f_{\rm prod} \propto \frac{1}{D(s)} \tag{14}$$

with the same denominator but a constant numerator [24]. The justification is that left-hand singularities due to coupling of σ to $\omega J/\Psi$ are very distant. The question is whether the Adler zero is needed in the amplitude for fitting KLOE data or not.

An interesting intermediate case is the production of the $\pi\pi$ S-wave in $\Upsilon' \to \Upsilon\pi\pi$. Recent BELLE data determine $\pi\pi$ mass spectra for the transitions $4S \to 1S$, $3S \to 1S$ and $2S \to 1S$ [25]. The first and last follow elastic scattering closely. The transition $3S \to 1S$ deviates from this and shows a peak towards the $\pi\pi$ threshold, reminiscent of that observed in $J/\Psi \to \omega\sigma$, where the Adler zero is absent. The combined mass of $\Upsilon(3S)$ and 2π lies close to the $B\bar{B}$ threshold, and Moxhay suggests that the decay proceeds through coupling to $B\bar{B}$ intermediate states [26]. These data suggest that for small momentum transfers the Adler zero is needed in the amplitude unless there is a flavour change. From Fig. 1 for ϕ radiative decays, it is plausible that the right-hand vertex should be the same as that in the on-shell $KK \to \pi\pi$ process, since the kinematics are similar. It will be shown that this successfully fits the data.

2.4 $\rho \to \eta\gamma$ and $\pi^0\gamma$

There are also amplitudes due to $\phi \to \pi^0\rho$, $\rho \to \eta\gamma$ and $\rho \to \pi^0\gamma$. Formulae for their intensities and interferences with a_0 or f_0 are given by Bramon et al. [27] and Achasov and Gubin [28]; a small correction to [28] for the intensity of $\phi \to \rho\pi$, $\rho \to \eta\gamma$ is made by Achasov and Kiselev [29]. Also equation (20) of [28] requires an additional factor $(m_\phi^2 - s)$ in the numerator; this correction is made in a second paper of Achasov and Kiselev [30] in their equation (21).

The $\rho\pi$ contribution to $\gamma(\pi^0\pi^0)$ peaks at $m_{\pi\pi} = 550$ MeV and is small. Interferences with $f_0(980)$ have rather little effect on the fit to $\gamma\pi^0\pi^0$. However, the contribution of $\rho \to \eta\pi^0$ is quite significant in $\gamma(\eta\pi^0)$.

Branching fractions for these processes will now be discussed, starting with $\rho \to \pi^0\gamma$. Achasov et al. report $\Gamma(\rho \to \gamma\pi^0) = 73.5 \pm 11$ keV [31]. This agrees with the PDG average for $\Gamma(\rho^\pm \to \gamma\pi^\pm)$ of 68 ± 7 keV. The weighted average is 70 ± 6 keV. The PDG gives an average for $\Gamma(\phi \to \rho\pi + \pi^+\pi^-\pi^0)/\Gamma_{\rm total} = 0.151 \pm 0.009$. Dividing this by 3 for neutral final states and assuming it is all $\rho\pi$, the branching fraction of $\phi \to \rho\pi^0 \to \pi^0\pi^0\gamma$ is 2.4×10^{-5}.

The experimental groups apply cuts to remove $\phi \to \omega\pi^0$, $\omega \to \pi^0\gamma$. It is hard to estimate the fraction of $\rho\pi^0$ events which this removes; a sharp cut in the ρ line-shape at the quoted mass cut leaves $\sim 40\%$ of $\rho\pi^0$ events, i.e. a branching fraction of $\phi \to \pi^0\pi^0 \sim 0.96 \times 10^{-5}$. The uncertainty is not serious, since most events lie at low $\pi^0\pi^0$ masses and have little effect on the $f_0(980)$ peak.

The arithmetic for the $\rho\pi^0$ contribution to $\gamma(\eta\pi^0)$ goes similarly. The weighted mean of SND [31] and CMD2 [32] values for $\Gamma(\rho \to \gamma\eta)/\Gamma_{\rm total}$ is $(2.95 \pm 0.26) \times 10^{-4}$. Taking the $\phi \to \rho\pi^0$ branching fraction to be 0.151/3, as above, and using the KLOE branching fraction $\phi \to \gamma(\eta\pi^0) = 0.83 \times 10^{-4}$, the ratio $(\phi \to \rho\pi, \rho \to \gamma\eta)/(\phi \to {\rm all}\gamma\eta\pi^0) = 0.18 \pm 0.02$. These events do contribute significantly to the fit; interference with $\gamma a_0(980)$ is included.

2.5 Formulae for $\pi\pi \to KK$

There is a major question how to combine the amplitudes for $f_0(980)$ and the broad σ. Data on $\pi\pi$ elastic scattering from the Cern–Munich experiment and elsewhere show that phase shifts of $f_0(980)$ and σ add to a good approximation. Both go through 90° near 1 GeV and the phase shift for the full amplitude passes rapidly through 180° just below 1 GeV. A natural and successful way of describing this situation is the Dalitz–Tuan prescription [33], where S-matrices of the two components are multiplied:

$$S_{\rm total} = S_A S_B = \eta_A \eta_B e^{{\rm i}(\delta_A + \delta_B)} \, . \tag{15}$$

However, it is not obvious that it is right to multiply elasticities.

An alternative approach is to use the K-matrix. It is conventional to add K-matrix elements for the two components [12]. The penalty in this approach is that each K-matrix pole appears where the total phase goes through 90°; the $f_0(980)$ is then described as a delicate interference between two poles displaced substantially from 1 GeV. In the present work that is inconvenient, since $f_0(980)$ is the focus of attention in ϕ decays; a formula is needed to parametrise it directly. Furthermore, it is not obvious that Nature chooses to add K-matrix elements.

Since $K \propto \tan\delta$, an alternative choice is

$$K_{\rm total} = \frac{K_A + K_B}{1 - K_A K_B} \tag{16}$$

so that phases again add below the KK threshold. However, this alternative fails to fit $\pi\pi \to KK$ data immediately above the KK threshold. This is because inelasticity of the σ amplitude grows fairly slowly above threshold, so (16) demands a rather elastic amplitude there.

One cannot add inelasticities of $f_0(980)$ and σ, since this leads to values outside the unitary circle. The approach adopted here is pragmatic. The Dalitz–Tuan prescription is simple, fits the phase of elastic scattering ade-

quately, predicts a reasonable result for the elasticity parameter η and successfully fits the data. The η parameter for the BES $f_0(980)$ drops precipitously to $\eta = 0.27$ at 1.01 GeV and then rises again (see Fig. 11a below). Since $f_0(980)$ and σ are approximately in phase, it seems likely that the effect of the σ component will be to increase the inelasticity to a value somewhere between 0 and the value for $f_0(980)$ alone. In practice, multiplying the S-matrix elements for S_{11} and S_{22} describes the data well up to 1.2 GeV, obtaining S_{12} from the exact relation

$$2|S_{12}|^2 = 1 + |S_{33}|^2 - |S_{11}|^2 - |S_{22}|^2 \,, \tag{17}$$

where indices 1,2,3 refer to $\pi\pi$, KK and $\eta\eta$. Note, however, that S_{12} itself does not factorise into $f_0(980)$ and σ components. This is a symptom of extensive multiple scattering. It may well be that there is no simple formula which fully describes strong coupling of the two amplitudes.

Above 1.2 GeV, the appearance of $f_0(1370)$, $f_0(1500)$ and $f_0(1790)$ makes the treatment via the Dalitz–Tuan prescription intractable. There, amplitudes are small enough that unitarity corrections are less than normalisation errors, and it is adequate to add amplitudes. That is the procedure adopted here, making a smooth join at 1.17 GeV using Lagrange multipliers to ensure that the magnitude and phase join continuously. For the $\eta\eta$ channel, amplitudes are so small that unitarity plays no significant role, so one can add amplitudes.

At the higher masses, $f_0(1370)$, $f_0(1500)$ and $f_0(1790)$ overlap significantly. The overlap makes the phase of the background below each resonance a sensitive parameter. In order to achieve a satisfactory fit, it is necesssary to multiply each amplitude by a fitted phase factor $\exp(i\theta)$ and add amplitudes.

In summary, multiplying η parameters near threshold puts a lower bound on the intensity 92% of the unitarity limit, and reduces the normalisation uncertainty from 50 to 8%. At higher masses, the amplitude is fitted freely in terms of known resonance, ignoring possible multiple scattering from one resonance to another where they overlap. This allows maximum freedom to fit σ and $f_0(980)$, the main object of the present work.

An important point is that the $f_0(980)$ signal appears as a sharp dip in elastic scattering, because phases add. In ϕ radiative decays, it appears as a peak. In this case, it is appropriate to add amplitudes, since they are weak and the unitarity limit imposes no significant constraint; in elastic scattering, the amplitude must follow the unitarity limit up to the KK threshold.

2.6 The 4π channel

Both $\pi\pi \to KK$ and $\pi\pi \to \eta\eta$ cross sections drop fairly rapidly with increasing mass, and almost disappear above 1.9 GeV. To some extent, this is due to competition from the 4π channel. Unfortunately, there are almost no data on the 4π channel, so the s-dependence of this inelasticity is poorly known. As in the work of Bugg, Sarantsev and Zou in 1996 [13], 4π phase space is parametrised empirically by a formula close to a Fermi function:

$$\rho_4(s) = \frac{\sqrt{1-16m_\pi^2/s}}{1-\exp[\Lambda(s_0-s)]} \,. \tag{18}$$

Here $\Lambda = 2.85\ \mathrm{GeV}^{-2}$ and $s_0 = 2.5\ \mathrm{GeV}^2$. This function approximates closely the onset of $\rho\rho$ and $\sigma\sigma$ final states.

2.7 The $\pi\pi$ S-wave

The propagator of the broad σ amplitude is written in (20) as the sum of contributions from $\pi\pi$, KK, $\eta\eta$ and 4π, labelled 1–4. In the first three, the Adler zero is accomodated in (21) by a factor

$$A(s) = (s - s_A)/\left(M^2 - s_A\right) \,, \tag{19}$$

where $s_A = (0.41 \pm 0.06)m_\pi^2$. The factor 0.41 comes from the work of Leutwyler and Colangelo, using chiral perturbation theory [34]. A form factor $FF_i^2(s) = \exp(-\alpha k_i^2)$ is included into channels 2 and 3 (KK and $\eta\eta$) in (22) and (23). Note that $FF_i(s)^2$ is multiplying the intensity of the KK channel, which is the quantity appearing in the width of the σ. It is required to parametrise the rapid drop of cross sections with increasing mass. The same α is used for both channels; k_i is the centre of mass momentum in each channel. The propagator is then written:

$$\begin{aligned}
D(s) &= M^2 - s - g_1^2 z_{\rm sub} - m(s) \\
&\quad - i\left[g_1^2\rho_1 + g_2^2\rho_2 + g_3^2\rho_3 + g_4^2(s)\right] && (20)\\
g_1^2 &= B_1 \exp\left[-(s-M^2)/B_2\right] A(s) && (21)\\
g_2^2 &= r_2 g_1^2 FF_2^2(s) && (22)\\
g_3^2 &= r_3 g_1^2 FF_3^2(s) && (23)\\
FF_i(s) &= \exp\left(-\alpha_i k_i^2\right) && (24)\\
g_4^2 &= B_4\rho_{4\pi}(s)/\rho_{4\pi}(M^2) && (25)\\
z(s) &= \frac{1}{\pi}\left[2 + \rho_1 \ln_{\rm e}\left(\frac{1-\rho_1}{1+\rho_1}\right)\right] && (26)\\
z_{\rm sub} &= z(s) - z(M^2) && (27)\\
m(s) &= \frac{s-M^2}{\pi}\int \frac{M\Gamma_{\rm tot}(s')\,{\rm d}s'}{(s'-s)(s'-M^2)} \,. && (28)
\end{aligned}$$

For other resonances, the exponential of (21) and the form factors FF are superfluous because the resonances are narrow; they are simply omitted, but the dispersive term $m(s)$ is retained. The amplitude for $\pi\pi$ elastic scattering is

$$\begin{aligned}
T_{11} &= 1 + 2iS_{11} && (29)\\
S_{11} &= \eta\exp(2i\delta) = g_i^2\rho_1/D(s) \,. && (30)
\end{aligned}$$

In fitting elastic data, S-matrices from σ, $f_0(980)$, $f_0(1370)$, $f_0(1500)$ and $f_0(1790)$ are multiplied together.

The function $g_1(s)$ was introduced by Zou and Bugg [35]. It takes a very simple empirical form which succeeds in fitting the broad S-wave over the whole mass range from threshold to 1.9 GeV using just the Adler zero (taken from other work) and three fitted parameters B_1,

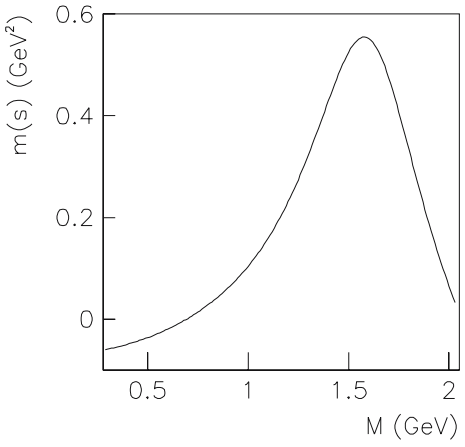

Fig. 2. The dispersive term $m(s)$ for the 4π channel

B_2 and M. At the KK and $\eta\eta$ thresholds, $r_2 = g^2_{KK}/g^2_{\pi\pi}$ and $r_3 = g^2_{\eta\eta}/g^2_{\pi\pi}$.

The motivation for the formalism is to make amplitudes fully analytic. This has been achieved below the region of strong 4π elasticity by Achasov and Kiselev [30]. Here the opening of the strong 4π channel is treated analytically for the first time. This will be important in demonstrating the presence of $f_0(1370)$; otherwise, the issue of analyticity turns out not to be crucial for present work. The function $z(s)$ accounts analytically for the opening of $\pi\pi$ phase space $\rho_1(s)$; it is taken from the work of Leutwyler and Colangelo [34]. It has the good feature of eliminating the divergence at $s = 0$ due to $\sqrt{1/s}$ in $\rho_1(s) = \sqrt{1 - 4m_\pi^2/s}$. In (27), a subtraction is made at $s = M^2$, where the real part of the S-wave amplitude goes to zero.

The term $m(s)$ is a dispersive contribution to the real part of the amplitude, allowing for the inelasticity in all channels. The inelasticity in 4π is large and gives rise to a slowly varying dispersive term illustrated in Fig. 2. It is far too wide to be confused with $f_0(1370)$, $f_0(1500)$ or $f_0(1790)$. The dispersive term $m(s)$ is also included into the Breit–Wigner forms for $f_0(1370)$, $f_0(1500)$ and $f_0(1790)$, again with a subtraction on resonance. This is important for $f_0(1370)$, where $\Gamma_{4\pi}$ is dominant.

One new result arises concerning the position of the σ pole. Fitting it with the new fully analytic formulae described above moves its pole position to $(506 \pm 30) - i(238 \pm 30)$ MeV from the BES value of $(541 \pm 39) - i(252 \pm 42)$ MeV [36]. The shift arises from the elimination of the singularity at $s = 0$ and dispersive corrections to the $\pi\pi$ channel. It is within the experimental errors, which now go down because of better control over the extrapolation to the pole.

3 Fit to $\phi \to \gamma(\eta\pi^0)$

If parameters of $a_0(980)$ are fitted directly to $\phi \to \gamma\eta\pi^0$ data of [5], the problem is that the upper side of the resonance is not visible, resulting in values of M, $g^2_{\eta\pi}$ and g^2_{KK} which are strongly correlated.

Most determinations quoted by the PDG have been obtained by fitting simple Breit–Wigner line-shapes with constant width to $\eta\pi$ or KK alone. These are of no use for present purposes, since they ignore the cusp at the KK threshold. A rather precise determination, not quoted by the PDG, was made in [8], combining data on $\bar{p}p \to \omega(\eta\pi^0)$ and $\bar{p}p \to (\eta\pi^0)\pi^0$ at rest. Both have high statistics (280 K events for $\eta\pi^0\pi^0$) and very low experimental backgrounds. The first reaction is dominated by $\omega a_0(980)$. Although a simple Breit–Wigner of constant width was fitted, the data determine precisely the location of the a_0 peak at half-height; the error quoted on the central mass is $1.23(\text{stat}) \pm 0.34(\text{syst})$ MeV and for the width is $0.34(\text{stat}) \pm 0.12(\text{syst})$ MeV. Those constraints go a long way towards breaking the correlation between couplings to $\eta\pi$ (which dominates the lower side of the resonance) and KK (which dominates the upper side). In $\eta\pi^0\pi^0$, the $a_0(980)$ appears very conspicuously in the Dalitz plot as an 'edge' at the KK threshold; at this edge, the phase turns abruptly by 90° in the Argand diagram. The a_0 interferes with the broad σ in the $\pi\pi$ channel. This interference determines rather precisely the phase variation of the a_0 as a function of $\eta\pi$ mass. On the other hand, there is some uncertainty in the parametrisation of the σ as a function of $\pi^0\pi^0$ mass. Taking into account all uncertainties, quoted parameters are $M = 999 \pm 5$ MeV, $g^2_{\eta\pi} = 221 \pm 20$ MeV and $r = g^2_{KK}/g^2_{\eta\pi} = 1.16 \pm 0.18$.

The fit to KLOE data with these parameters immediately reproduces the line-shape accurately. The fitted normalisation is low by 32%, which is close to the combined errors, as follows. From $g^2_{\eta\pi}$, there is an error of 19% in the magnitude predicted for KLOE data, and from r

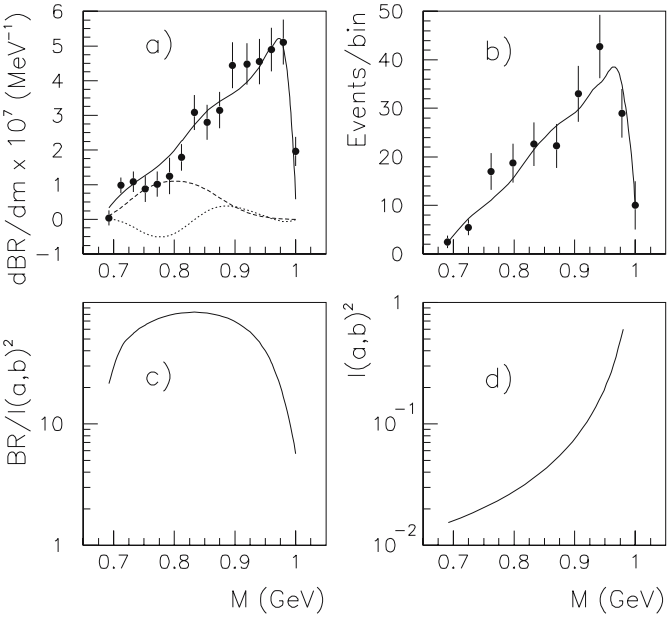

Fig. 3. The fit to KLOE data [5] where **a** $\eta \to \gamma\gamma$, **b** $\eta \to 3\pi$; in **a**, *dashed* and *dotted curves* show the $\varrho\pi$ contribution and interference with $a_0(980)$; **c** the energy dependent factor appearing in $\mathrm{d}\Gamma/\mathrm{d}m$, but omitting $|I(a,b)|^2$, **d** $|I(a,b)|^2$ itself

there is a further error of 15%. The error quoted by the PDG for the normalisation of $\phi \to \gamma\eta\pi$ is 6%. To achieve agreement in normalisation, it is necessary to stretch all parameters by 1σ as follows. For a_0, $g^2_{\eta\pi}$ has been increased to 241 MeV, and $r = g^2_{KK}/g^2_{\eta\pi}$ to 1.34; this requires reoptimising $M = 991.5$ MeV. The branching fraction of $\rho \to \eta\pi$ has been increased to 0.20 and the normalisation of KLOE data has been decreased by 6%. The final fit is shown in Fig. 3a and b. Dashed and dotted curves show the intensity of the $\rho \to \eta\pi$ signal and its interference with $a_0(980)$. A minor detail is that a form factor $\exp -\beta k^2_\gamma$ is included to allow for the charge radius of the kaon, 0.560 fm [16].

Figure 3c and d illustrate the strong energy-dependent factors contributing to the intensity. Figure 3d shows $|I(1,b)|^2$ from the KK loop. It falls dramatically as the kaons go off the mass-shell. Figure 3c illustrates the remaining factors from $mk^3_\gamma \rho_{\eta\pi}$, (2). These factors inflate the lower side of $a_0(980)$. The agreement with the a_0 parameters of [8] for both line-shape and normalisation confirms Achasov's KK loop model at the level of $\sim 15\%$ in amplitude. That conclusion will be important in considering the $\gamma\pi^0\pi^0$ data.

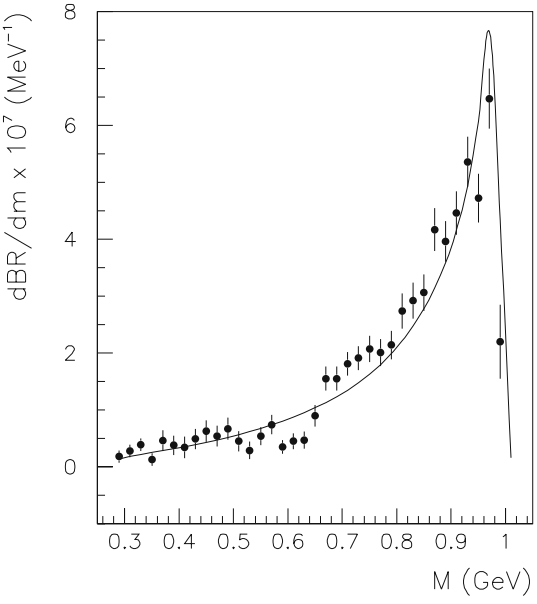

Fig. 4. Fit to KLOE $\gamma(\pi^0\pi^0)$ data with $f_0(980) + \varrho\pi$ when the normalisation is floated

4 Fit to $\phi \to \gamma(\pi^0\pi^0)$

KLOE data on $\phi \to \gamma(\pi^0\pi^0)$ [4] can be fitted fairly well with BES parameters for $f_0(980)$ if the absolute normalisation is floated, see Fig. 4. The best fit is obtained by fitting the form factor FF freely and stretching BES parameters to the limits of their quoted statistical and systematic errors as follows: $M = 0.957$ GeV, $g^2_1 = 0.190$ GeV, $g^2_2/g^2_1 = 3.75$. However, $\chi^2 = 122$, compared with 60 for the fit shown later in Fig. 6 including $\sigma \to KK$. The data are taken from Fig. 4 of the KLOE publication [4] after subtracting their estimated background; they are not taken from their Table 5, where the background has been unfolded in such a way as to accomodate a dip near 520 MeV.

There is however a serious problem with the absolute normalisation. The fit with $f_0(980)$ alone has a normalisation at least a factor 2 lower than the data. The program is identical to that used for $\gamma\eta\pi^0$ except for trivial changes in the parameters of the Breit–Wigner amplitude and the change from the mass of the η to the π^0. A direct comparison of the relative normalisation of $\gamma\pi^0\pi^0$ and $\gamma\eta\pi^0$ has been made using (10).

A variety of explanations for the normalisation are possible, but look odd in view of the agreement in normalisation for $\gamma\eta\pi^0$ data. Firstly, Oller remarks that there may be a contact term involving two K^0 in the loop diagram, and a photon radiated from the ϕ decay vertex [37]. Secondly, Oset and collaborators have suggested that ϕ may decay through intermediate states involving K^*K, where K^* may be $K^*(890)$, $K_1(1270)$ or $K_1(1400)$ [38].

A further alternative is proposed here. This is that the broad σ couples to the KK loop. It will be shown in Section 5 that data on $\pi\pi \to KK$ require this broad component. Independent support is available from the work of Büttiker, Descotes-Genon and Moussallam [39]. They apply the Roy equations to fitting data on $\pi K \to \pi K$ and $\pi\pi \to KK$. For the present discussion, this corresponds to calculating the $\pi\pi \to KK$ amplitude below the KK threshold as a continuation of the amplitude above threshold using (i) the dispersion integral over the physical $\pi\pi \to KK$ process, (ii) nearby pole terms due to t and u-channel exchanges of $\rho(770)$ and $K^*(890)$. Their Fig. 12, reproduced here as Fig. 5, shows the magnitude $|g^0_0|$ of their $\pi\pi \to KK$ amplitude both above and below the KK threshold. The $f_0(980)$ signal is superimposed on a strong broad component. Achasov and Kiselev [29] similarly include coupling of σ to KK, but they fit parameters of $f_0(980)$ freely.

For the fit presented here, the $f_0(980)$ contribution is fixed in magnitude to BES parameters. The charge form factor of the photon to KK is fitted freely. The magnitude of $\sigma \to KK$ optimises with a threshold ratio $r_2 = g^2_{KK}/g^2_{\pi\pi} = 0.6 \pm 0.1$. Its phase with respect to $f_0(980)$ requires some comment. The production process is electromagnetic, and will produce a phase shift only of order $\alpha = 1/137$. In $\pi\pi$ elastic scattering, both σ and $f_0(980)$ have a phase shift of $\sim 90^\circ$ at 990 MeV. Their relative phase is constrained in fitting KLOE data within $\pm 10^\circ$, the combined error from σ phases and the mass of $f_0(980)$. It fits naturally at the edge of this band; if the constraint is removed, χ^2 changes by only 2 and the fit hardly changes.

The resulting fit is shown in Fig. 6a. Panel b displays the $f_0(980)$ intensity as the full curve, the σ as the dashed curve and the interference between them as the dotted curve. Panel c shows the fitted $\rho\pi$ signal (full curve) compared with data at low masses. Its magnitude is fixed according to the arithmetic of Sect. 2.4. A marginal improvement may be obtained by fitting it freely, but there is no significant effect on the fitted σ amplitude.

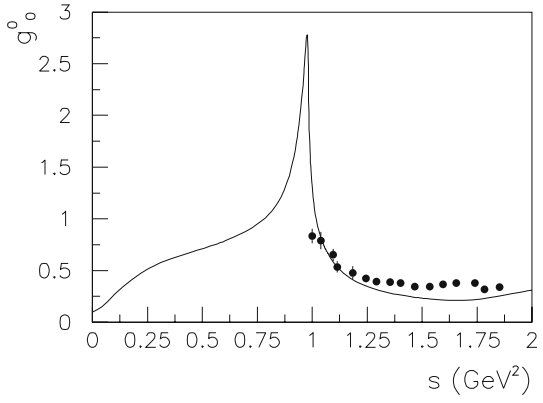

Fig. 5. The magnitude of the $\pi\pi \to KK$ amplitude from Büttiker et al. [39] fitted using the Roy equations and experimental data of Cohen et al. [40]

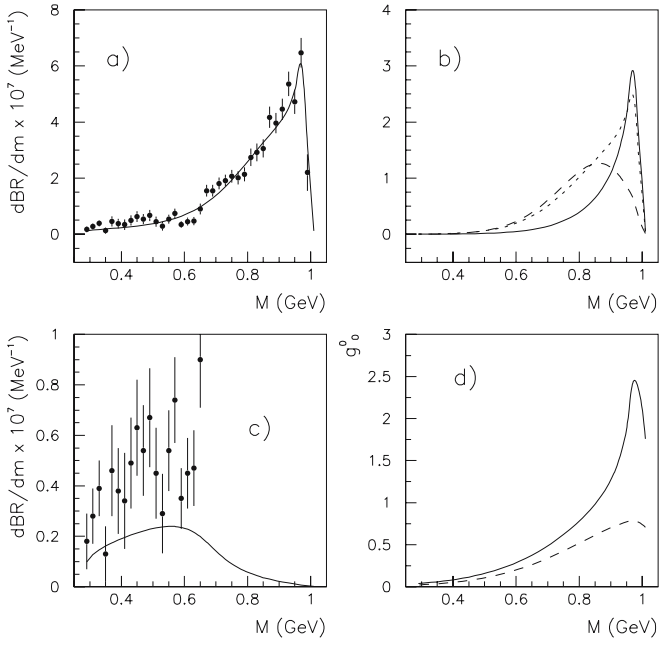

Fig. 6. a Fit to KLOE $\gamma\pi^0\pi^0$ data after background subtraction; **b** contributions from $f_0(980)$ (*full curve*), σ (*dashed*) and interference (*dotted*); **c** an enlarged view of the contribution from $\varrho\pi$, $\varrho \to \gamma\pi^0$; **d** $|g^0_0|$ from my fit (*full curve*) and the contribution from σ alone (*dashed*)

Figure 6d shows $|g^0_0|$ from my fit to $\pi\pi \to KK$ as the full curve. The peak due to $f_0(980)$ is slightly lower than that in Fig. 5 because the $f_0(980)$ of BES is slightly broader than that of Büttiker et al. Secondly, the fit requires a fairly strong form factor to cut off the lower sides of both $f_0(980)$ and σ. It is parametrised as $\exp -8.4k^2_\gamma$, where k is in GeV. Comments on the origin of this factor will be given in Sect. 4.1.

For completeness, Fig. 7 shows fits to Novosibirsk data on $\phi \to \gamma(\eta\pi^0)$ and $\gamma\pi^0\pi^0$. The point in $\gamma(\eta\pi^0)$ at 0.98 GeV is clearly too high and is slightly inflating the PDG average for the branching ratio $\phi \to \gamma(\eta\pi^0)$.

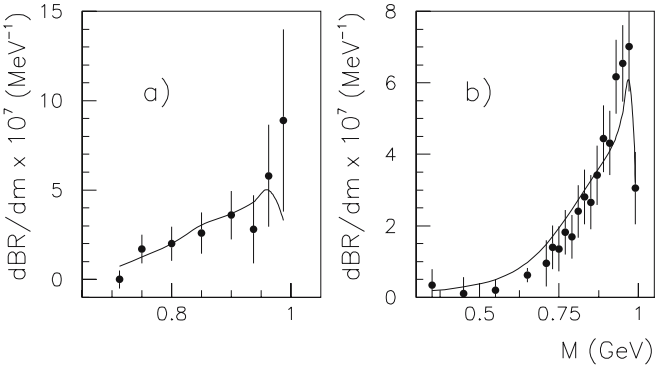

Fig. 7. Fits to Novosibirsk data on $\phi \to \gamma(\eta\pi^0)$ [2] and $\phi(\pi^0\pi^0)$ [3]

4.1 Sensitivity to fitting parameters

The heights of the peaks at 970 MeV in both $\gamma(\eta\pi^0)$ and $\gamma(\pi^0\pi^0)$ have limited sensitivity to resonance parameters. In the denominators $D(s)$, $g^2_{\pi\pi}\rho_{\pi\pi}$ or $g^2_{\eta\pi}\rho_{\eta\pi}$ appear in the imaginary part, while M and $g^2_{KK}\sqrt{4M^2_K/s-1}$ appears in the real part. There is considerable compensation between the numerator $N(s)$ and denominator $D(s)$ of the Breit–Wigner amplitudes. For $\gamma(\eta\pi^0)$, it is necessary to constrain the location of the a_0 peak at half-height within, say, 2 or 2.5 standard deviations of the values quoted in Section 3, adding statistical and systematic errors linearly. With this constraint, M, $g^2_{\eta\pi}$ and g^2_{KK} may be varied freely. Because of the feedback between $N(s)$ and $D(s)$, it is only just possible to accomodate the 32% discrepancy by including also flexibility in the $\rho\pi$ contribution and uncertainty in the KLOE normalisation.

For $f_0(980)$, the BES $\pi\pi$ peak must again be constrained in mass and the full width must be constrained to 34 ± 4 MeV. There is more flexibility in g^2_{KK}, since the BES $f_0(980) \to KK$ signal interferes with a background due to $\sigma \to KK$; the error on g^2_{KK}, namely $\pm 0.25(\text{stat}) \pm 0.21(\text{syst})$ quoted by BES, represesents one standard deviation. It turns out that with this flexibility, the absolute normalisation of the $f_0(980)$ peak cannot change by more than $\pm 15\%$. Some fits reported in the literature have changed $g^2_{\pi\pi}$ and $g^2_{KK}/g^2_{\pi\pi}$ by factors of 2; that is unrealistic.

The peak at 970 MeV in KLOE data determines the magnitude of the background amplitude there. The fit is not unduly sensitive to the parametrisation of $\pi\pi$ phase shifts. What matters for $\gamma(\pi^0\pi^0)$ is only the way the σ and $f_0(980)$ amplitudes go out of phase off resonance. Any form which reproduces $\pi\pi$ phase shifts within errors of, say, $\pm 4^\circ$ is adequate. The full apparatus of (18)–(30) has been used to scrutinise the combined fit with $\pi\pi \to \pi\pi$, KK and $\eta\eta$. An equivalent and more convenient form which fits all the data equally well may be obtained by (i) dropping the dispersive contribution $m(s)$ completely, (ii) also the tiny contribution from the 4π channel below the KK threshold, (iii) replacing the effect of $m(s)$ for KK and $\eta\eta$ below their thresholds by a form factor $\exp(-5.2|k^2_K|)$, with

k_K in GeV/c. Then $M = 0.7366\,\mathrm{GeV}$, $B_1 = 0.6470\,\mathrm{GeV}^2$, $B_2 = 4.271\,\mathrm{GeV}^2$, $B_4 = 0.00221\,\mathrm{GeV}^2$. Values of other parameters will be discussed below but will be collected here for convenience of reference: $r_3 = 0.20$, $r_2 = 0.6$.

A crucial parameter in fitting $\sigma \to KK$ in KLOE data is the form factor of (24), $FF = \exp(-8.4k_\gamma^2)$, where k_γ is in GeV. Without this factor, the background amplitude is too large at low mass; one can see this in the difference between Figs. 5 and 6d. This form factor has at least three possible origins.

Firstly, it may be due to the size of the KK cloud. This would require an RMS radius of 1.4 fm. It is well known that a source of finite size produces a form factor $\sin(kr)/kr = 1 - k^2r^2/6 + \ldots$. The second sheet pole of $f_0(980)$ lies at $(998 \pm 4) - i(17 \pm 4)\,\mathrm{MeV}$. The binding energy is so close to the KK threshold that the $f_0(980)$ inevitably has a KK cloud of roughly this size, resembling the long-range tail of the deuteron. The pole for $a_0(980)$ is much further away, at 1032–i85 MeV, so the RMS radius of $a_0(980)$ has conventional dimensions and a weaker form factor.

A second straightforward possibility is that $f_0(980)$ and the broad σ component mix over the mass range where they are both large. This mixing will be confined naturally to their region of strong overlap.

A third possibility is that $|g_0^0|$ fitted by Büttiker et al. has some flexibility in the range $s = 0.2$–$0.8\,\mathrm{fm}$. It is well constrained near 1 GeV, and also for $s = -0.5$ to $0\,\mathrm{GeV}^2$ (by data on $\pi K \to \pi K$). In between, Adler zeros in $\pi\pi$ at $s \sim 0.5m_\pi^2$ and in coupling to KK at $s \sim 0.5m_K^2$ may pull $|g_0^0|$ down. Data on $\phi \to \gamma(\pi^0\pi^0)$ appear to be the only data directly sensitive to this possibility.

5 Fits to $\pi\pi \to KK$ and $\eta\eta$

5.1 Introduction

A problem with data on $\pi\pi \to KK$ is that cross sections from different experiments differ in normalisation by up to a factor 2. This problem is minimised here by using the BES parameters for $f_0(980)$ to assist the absolute normalisation. All $\pi\pi \to KK$ data are rescaled to the BES normalisation. However, one can still not rely on $\pi\pi \to KK$ data to separate branching fractions of $f_0(1370)$, $f_0(1500)$ and $f_0(1790)$ to KK and $\eta\eta$. Vastly better determinations are available from the analysis of Crystal Barrel data on $\bar{p}p$ annihilation at rest to $3\pi^0$, $\eta\pi^0\pi^0$, $\eta\eta\pi^0$ and several $KK\pi$ charge combinations. All of these data have been fitted self-consistently by Sarantsev and collaborators; decay widths to $\pi\pi$ and $\eta\eta$ are taken from this analysis [41]. Their errors are used to set limits within which parameters may vary; Table 1 shows these limits and values at which they optimise. Note however, that the present data really only determine the products $\Gamma_{\pi\pi} \times \Gamma_{KK}$ and $\Gamma_{\pi\pi} \times \Gamma_{\eta\eta}$. Values of $\Gamma_{4\pi}$ are determined from $\Gamma_{4\pi} = \Gamma_{\mathrm{total}} - \Gamma_{\pi\pi} - \Gamma_{KK} - \Gamma_{\eta\eta}$ at each resonance mass.

Some comments are needed on $f_0(1370)$ and $f_0(1790)$. There has been some unnecessary controversy recently concerning the existence of $f_0(1370)$, so its properties will be outlined briefly; it will be the subject of a separate publication giving full details from latest analyses of Crystal Barrel data. It appears most clearly in $\bar{p}p \to 3\pi^0$, where it is statistically at least a 50 standard deviation signal. Statistics are 600K events, with almost no experimental background. In early analyses of these data, there was some sensitivity to the parametrisation of the $\pi\pi$ S-wave amplitude, with which it interferes. The behaviour of the broad S-wave amplitude is now known much better.

The $f_0(1370)$ decays dominantly to 4π with $\Gamma(\pi\pi)/\Gamma(4\pi) \leq 0.2$. The 4π inelasticity increases rapidly with mass, so it is essential to treat the s-dependence of this width fully. The result is that the $\pi\pi$ signal peaks at $1320 \pm 30\,\mathrm{MeV}$, as in the analysis of Anisovich et al. [41]. The 4π channel peaks approximately 75 MeV higher, because of the rapidly expanding phase space. The apparent width in $\pi\pi$ and 4π channels is likewise different. PDG listings assign unreasonably large errors because these facts have not been taken into account in most analyses. The s-dependence of the 4π width is taken into account here, including the associated dispersive correction to $m(s)$ in the Breit–Wigner amplitude.

In elastic scattering, the intensity of $f_0(1370)$ is $< 4\%$ of the unitarity limit. It is swamped by the $f_2(1270)$, which has a spin multiplicity 5 times larger. Achasov and Shestakov point out a rather large error in $\Gamma_{4\pi}$ for $f_2(1270)$ [42]. This adds to the difficulty of normalising Cern–Munich moments in the region of $f_0(1370)$.

The $f_0(1790)$ is required as well as $f_0(1710)$ by recent BES data. The $f_0(1710)$ appears clearly in $J/\Psi \to \omega K^+K^-$ [43]. It is conspicuously absent in $J/\Psi \to \omega\pi^+\pi^-$ [36]. Those two sets of data require $\pi\pi/KK < 0.11$ for $f_0(1710)$ with 95% confidence. In $J/\Psi \to \phi\pi^+\pi^-$, there is a distinct $\pi\pi$ signal at 1790 MeV, but no significant signal in ϕK^+K^- [10]. The branching fraction $\pi\pi/KK$ is a factor 25 larger than allowed for $f_0(1710)$, hence requiring a separate resonance $f_0(1790)$. There was previous ev-

Table 1. Limits used in the fit (in MeV); optimised values are in parentheses

State	$f_0(1370)$	$f_0(1500)$	$f_0(1790)$
M	1290–1335 (1290)	1495–1510 (1501)	1770–1800 (1800)
Γ_{total}	200–280 (280)	110–135 (135)	180-280 (280)
$\Gamma_{\pi\pi}$	34-58 (48)	35–39 (35)	30–100 (72)
$\Gamma_{KK}/\Gamma_{\pi\pi}$	0.04–0.235 (0.235)	0.22–0.272 (0.272)	0.16–1.2 (0.47)
$\Gamma_{\eta\eta}/\Gamma_{\pi\pi}$	0.08–0.18 (0.18)	0.04–0.18 (0.11)	0.1–1.0 (0.20)

idence for it in $J/\Psi \to \gamma 4\pi$ [44,45] and $\bar{p}p \to \eta\eta\pi^0$ [46]. Here, both $f_0(1710)$ (with its upper limit for $\pi\pi$ coupling) and $f_0(1790)$ (with its upper limit for KK coupling) are included. However, the present data do not distinguish cleanly between them.

5.2 $\pi\pi \to \eta\eta$

Figure 8 shows fits to $\pi\pi \to KK$ data and $\eta\eta$. The fit to $\eta\eta$ in panel d will be discussed first, since it is simple and concerns only one set of data, from GAMS [47]. The normalisation is such that the unitarity limit is at an intensity of 0.25; this arises from the relation $T_{12} = S_{12}/2i$ between T and S-matrices. The full curve shows the overall fit, including contributions from σ (dotted curve), $f_0(1370)$, $f_0(1500)$ and $f_0(1790)/f_0(1710)$. The main features are a gradually falling $\sigma \to \eta\eta$ signal and destructive interference with $f_0(1500)$, which is mainly responsible for the dip at 1.45 GeV. The peak at higher masses comes from $f_0(1500)$ interfering with $f_0(1710)$ and $f_0(1790)$. The Argand diagram is shown in Fig. 9b.

The fitted ratio $r_3 = g_3^2/g_1^2$ at the $\eta\eta$ threshold is 0.20 ± 0.04. The error arises from normalisation uncertainty and a possible weak coupling of $f_0(980)$ to $\eta\eta$; an upper limit on this coupling is obtained from BES data on $J/\psi \to \phi\pi^+\pi^-$ and ϕK^+K^-, from the fact that no drop is observed at the $\eta\eta$ threshold in the $\pi\pi$ mass spectrum. This upper limit is $r_3 \simeq 0.33$.

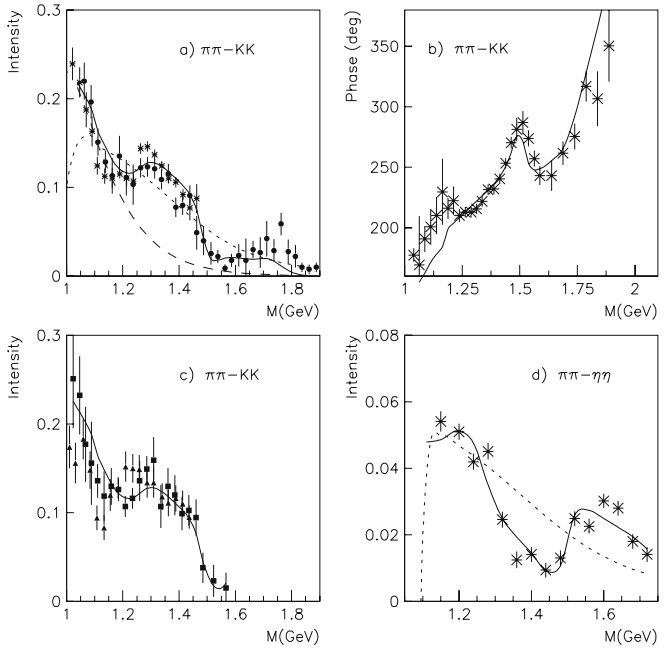

Fig. 8. **a** Fit to $\pi\pi \to KK$ (*full curve*); *circles* show data of Lindenbaum and Longacre [48] and *crosses* those of Martin and Ozmutlu [52]; the *dashed curve* shows the intensity of $f_0(980)$ and the *dotted curve* that from σ; **b** fit to phases of Etkin et al. [54]; **c** fit to the data of Cohen et al. [40] (*squares*) and Polychronakos et al. [53] (*triangles*); **d** fit to data of Binon et al. [47] for $\pi\pi \to \eta\eta$ (*full curve*); the *dotted curve* shows the σ contribution

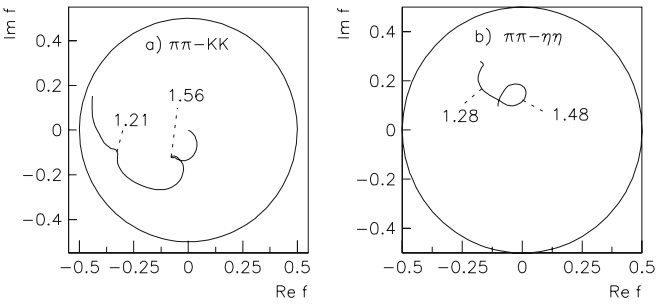

Fig. 9. Argand diagrams for **a** $\pi\pi \to KK$ and **b** $\pi\pi \to \eta\eta$; masses are marked in GeV

5.3 $\pi\pi \to KK$

It is first necessary to review the many available sets of data. It is important to realise that an analysis of moments was required in order to separate spins $J = 0$, 1 and 2 and small amounts of higher J. The papers make clear that there is some cross-talk with the high mass tail of $\rho(770)$ and with $f_2(1270)$, whose branching ratio to KK is not particularly well known.

Costa et al. [50] produced data on $\pi^- p \to K^+K^-n$, but found 8 alternative solutions, because of ambiguities over the exchange process and the possibility of both $I = 1$ and 0 contributions to the final state. Cason et al. [51] produced data on $\pi^- p \to K_S^0 K_S^0$ and observed a shoulder at 1300 MeV. They obtained two solutions, one with a narrow S-wave resonance (width ~ 95 MeV) at this mass and the second with a more slowly varying amplitude similar to today's $f_0(1370)$. The situation clarified further with data from Pawlicki et al. [49] on both $\pi^- p \to K^+K^-n$ and $\pi^+ n \to K^-K^+p$. These data favoured the second solution of Cason et al. and assigned $I = 0$. A meticulous analysis of the t-dependence of data was made by Martin and Ozmutlu [52]. This analysis showed that π exchange dominates at low t, as expected. The paper of Polychronakos et al. [53] on $\pi^- p \to nK_S^0 K_S^0$ is a full length paper on the data of Cason et al. The publication of Cohen et al. [40] gives a revised partial wave analysis of the data of Pawlicki et al. and again favours a structure close to today's $f_0(1370)$. Etkin et al. [54] reported data on $\pi^- p \to K_S^0 K_S^0 n$. Further statistics were added in the paper of Lindenbaum and Longacre [48].

It is noteworthy that all the later sets of data [40, 48, 53] observed a definite small bump at 1300 MeV, which was christened the ϵ at the time and is now $f_0(1370)$. All also observed a threshold peak due to $f_0(980)$. However, there are discrepancies concerning the height of the $f_0(980)$ peak with respect to the 1300 MeV mass range. The analyses of Martin and Ozmutlu and Longacre et al. agree well. The revised analysis by Cohen et al. of the Pawlicki et al. data gives a distinctly lower $f_0(980)$ than that of Longacre et al. And the data of Polychronakos et al. give an even lower $f_0(980)$ peak.

To clarify the situation including today's information about $f_0(1370)$, the four sets of data from Lindenbaum and Longacre, Cohen et al., Martin and Ozmutlu and Polychronakos et al. were included into the inital stages of the

analysis reported here. This was despite the fact that those of Martin and Ozmutlu and Cohen et al. are based on the same actual data before the moments analysis. The objective is to see whether the analysis favours one or the other. This is not the case and the fit goes midway between the two, so they are both retained in the final fit, but with a weight half that of Longacre et al.

The final fit is shown in Fig. 8a and b. The $f_0(980)$ produces the threshold peak, but its tail at high mass cannot account for the remaining features. Some $\sigma \to KK$ is definitely required and the dotted curve shows the optimum fit. It requires a form factor $FF = \exp(-5.2k^2)$ with k is GeV/c. However, some of this form factor may reflect the effect of competition between KK and 4π channels. The $\eta\eta$ threshold contributes a drop in the intensity of 0.02 between 1.09 and 1.18 GeV. The $f_0(1370)$ helps fit the bump at 1300 MeV. Destructive interference with $f_0(1500)$ is required to fit the dip at 1550 MeV. The fit to the 1550–1900 MeV intensity is not perfect because of difficulties in reproducing the large phase variation reported by Etkin et al. [54]. The fit to their phases is shown in panel b. However, one should be aware that other phase determinations show systematic differences with their data: the whole curve can move up or down by up to 30°, although the trend of the phase with mass remains similar to Fig. 8b. These differerences probably arise from the way spin 2 is fitted in different analyses. Etkin et al. included $f_2'(1525)$, but at that time the existence of $f_2(1565)$ was not known, and could lead to small systematic shifts. Another possible source of systematic error is that the present fit ends at 1900 MeV; there may be some contribution from the known $f_0(2020)$ which is presently not fitted.

The optimum fit gives $r_2 = 0.6^{+0.1}_{-0.2}$, (22), in close agreement with the KLOE data. This value can depend systematically on the s-dependence fitted to $f_0(980)$ and on 4π inelasticity. The $f_0(980)$ is fitted with a conservative form factor $\exp(-2.7k^2)$, where k is kaon centre of mass momentum; this corresponds to a radius of 0.8 fm for the $\pi\pi \to KK$ interaction, i.e. a conventional radius. Figure 8c compares the fit with intensities derived by Cohen et al. [40] (squares) and those of Polychronakos et al. [53] (triangles). The latter are systematically low below 1.15 GeV, so they are omitted from the final fit.

Figure 10a shows the fit without $f_0(1370)$. It fails to fit the dip below 1300 MeV. Since that structure is observed

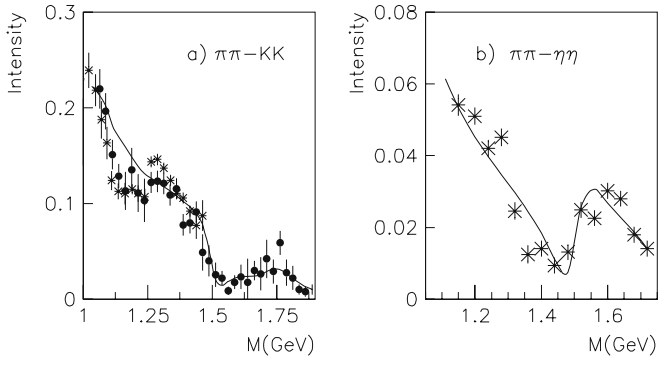

Fig. 10. Fits without $f_0(1370)$ for **a** $\pi\pi$, **b** $\eta\eta$

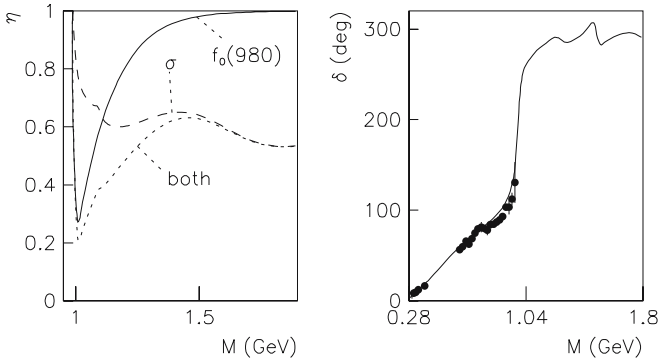

Fig. 11. a Contributions to elasticity η for $\pi\pi$ elastic scattering from $f_0(980)$ alone (*full curve*), σ (*dashed*) and their product (*dotted*). **b** Fitted $\pi\pi$ phase shifts; *points* show data of Pislak et al. [55] below 400 MeV and Cern–Munich data above 600 MeV [14]

in 3 experiments and 4 sets of data, it is hard to deny the presence of $f_0(1370)$; its fitted mass and width agree within errors with the best determinations from Crystal Barrel [41] and BES [10]. There is presently no alternative explanation of the 1300 MeV bump. The onset of 4π inelasticity is far too slow to account for structure with the width observed around 1300 MeV, and is anyway taken into account fully in the present analysis. Figure 10b also shows the change in fitting $\pi\pi \to \eta\eta$ when $f_0(1370)$ is removed; however, the points in Fig. 8d fluctuate around the fit by more than statistics, so it is difficult to estimate the significance of $f_0(1370) \to \eta\eta$.

Figure 11a illustrates the way elasticities of $f_0(980)$ and σ combine. The dotted curve shows the result obtained by multiplying $f_0(980)$ and σ contributions, according to the model assumed here. Figure 11b shows the phase shift fitted to $\pi\pi$ elastic scattering; errors above the $f_0(980)$ are typically $\pm 15°$.

6 Summary

Data on $\phi \to \gamma(\eta\pi)$ agree within errors in both absolute normalisation and mass spectrum with the parameters of $a_0(980)$ from [8]; the KLOE data suggest a normalisation which can be accomodated by shifting $a_0(980)$ parameter to $M = 991.5 \pm 4$ MeV, $g^2_{\eta\pi} = 0.241 \pm 14\,\mathrm{GeV}^2$, $g^2_{KK}/g^2_{\eta\pi} = 1.34 \pm 0.13$. The errors quoted here are reduced compared with [8] after the combined fit with KLOE data. The agreement with KLOE data suggests that the KK loop model is reliable. If BES parameters for $f_0(980)$ are used, data on $\phi \to \gamma(\pi^0\pi^0)$ have a normalisation higher than the fit by at least a factor 2. This discrepancy may be solved by allowing constructive interference between $f_0(980)$ and $\sigma \to KK$. The fit requires a ratio $r_2 = g^2(\sigma \to KK)/g^2(\sigma \to \pi\pi) = 0.6 \pm 0.1$ at the KK threshold. Data on $\pi\pi \to KK$ also require coupling of σ to KK with the same value of r_2 within experimental errors. Data on $\pi\pi \to \eta\eta$ require a ratio $r_3 = g^2(\sigma \to \eta\eta)/g^2(\sigma \to \eta\eta) = 0.20 \pm 0.04$ at the $\eta\eta$ threshold.

The interpretation of branching ratios in terms of models for $f_0(980)$, $a_0(980)$, σ and κ is discussed in an accompanying publication.

Acknowledgements. I am grateful to Dr. S. Giovanella for explaining technical points concerning KLOE data. I am grateful to Prof. H. Leutwyler for extensive discussions of how to fit the $\pi\pi$ S-wave amplitude with analytic functions. I wish to thank Prof. A. Sarantsev for discussion about the status and parameters of $f_0(1370)$. I also wish to thank Dr. C. Hanhart for valuable discussion on formulae.

References

1. M.N. Achasov et al., Phys. Lett. B **438**, 441 (1998); B **479**, 53 (2003)
2. R.R. Akhmetshin et al., Phys. Lett. B **462**, 380 (1999)
3. M.N. Achasov et al., Phys. Lett. B **440**, 442 (1998); B **485**, 349 (2000)
4. A. Aloisio et al., Phys. Lett. B **537**, 21 (2002)
5. A. Aloisio et al., Phys. Lett. B **536**, 209 (2002)
6. N.N. Achasov, V.N. Ivanchenko, Nucl. Phys. B **315**, 465 (1989)
7. M. Bolgione, M.R. Pennington, Eur. Phys. J. C **30**, 503 (2003)
8. D.V. Bugg, V.V. Anisovich, A.V. Sarantsev, B.S. Zou, Phys. Rev. D **50**, 4412 (1994)
9. C. Amsler et al., Phys. Lett. B **327**, 425 (1994)
10. M. Ablikim et al., Phys. Lett. B **607**, 243 (2005)
11. K.L. Au, D. Morgan, M.R. Pennington, Phys. Rev. D **35**, 1633 (1987)
12. A.V. Anisovich, V.V. Anisovich, A.V. Sarantsev, Zeit. Phys. A **359**, 173 (1997)
13. D.V. Bugg, A.V. Sarantsev, B.S. Zou, Nucl. Phys. B **471**, 59 (1996)
14. B. Hyams et al., Nucl. Phys. B **64**, 134 (1973)
15. F. Close, N. Isgur, S. Kumano, Nucl. Phys. B **389**, 513 (1993)
16. Particle Data Group (PDG), Phys. Lett. B **592**, 1 (2004)
17. D.V. Bugg, Phys. Lett. B **572**, 1 (2003)
18. E. Marco, S. Hirenzaki, E. Oset, H. Toki, Phys. Lett. B **470**, 20 (1999)
19. J.A. Oller, E. Oset, Nucl. Phys. A **620**, 438 (1997)
20. J.A. Oller, E. Oset, J.R. Pelaez, Phys. Rev. D **59**, 074001 (1999)
21. J.A. Oller, E. Oset, Phys. Rev. D **60**, 074023 (1999)
22. M. Jamin, J.A. Oller, A. Pich, Nucl. Phys. B **587**, 331 (2000)
23. A. Gomez Nicola, J.R. Pelaez, Phys. Rev. D **65**, 054009 (2002)
24. D.V. Bugg, Eur. Phys. J. C **37**, 433 (2004)
25. K. Abe et al., (BELLE), hep-ex/0512034
26. P. Moxhay, Phys. Rev. D **39**, 3497 (1989)
27. A. Bramon et al., Eur. Phys. J. C **26**, 253 (2002)
28. N.N. Achasov, V.V. Gubin, Phys. Rev. D **63**, 094007 (2001)
29. N.N. Achasov, A.V. Kiselev, Phys. Rev. D **68**, 014006 (2003)
30. N.N. Achasov, A.V. Kiselev, hep-ph/0512047
31. M.N. Achasov et al., hep-ex/0512027
32. R.A. Akhmetshin et al., Phys. Lett. B **509**, 217 (2001)
33. R.H. Dalitz, S. Tuan, Ann. Phys. (N.Y.) **10**, 307 (1960)
34. H. Leutwyler, G. Colangelo, private communication
35. B.S. Zou, D.V. Bugg, Phys. Rev. D **50**, 591 (1993)
36. M. Ablikim et al., Phys. Lett. B **598**, 149 (2004)
37. J.A. Oller, Nucl. Phys. A **714**, 161 (2003)
38. J.E. Palomar, L. Roca, E. Oset, M.J. Vicente Vacas, Nucl. Phys. A **729**, 743 (2003)
39. P. Büttiker et al., Eur. Phys. J. C **33**, 409 (2004)
40. D. Cohen et al., Phys. Rev. D **22**, 2595 (1980)
41. V.V. Anisovich, C.A. Nikonov, A.V. Sarantsev, Phys. Atom. Nucl. **65**, 1545 (2002)
42. N.N. Achasov, G.N. Shestakov, Phys. Rev. D **67**, 114018 (2003)
43. M. Ablikim et al., Phys. Lett. B **603**, 138 (2004)
44. D.V. Bugg et al., Phys. Lett. B **353**, 378 (1995)
45. J.Z. Bai et al., Phys. Lett. B **472**, 207 (2000)
46. A. Anisovich et al., Phys. Lett. B **449**, 154 (1999)
47. F. Binon et al., Nu. Cim. A **78**, 313 (1983)
48. S.J. Lindenbaum, R.S. Longacre et al., Phys. Lett. B **274**, 492 (1992)
49. A.J. Pawlicki et al., Phys. Rev. D **15**, 3196 (1977)
50. G. Costa et al., Nucl. Phys. B **175**, 402 (1980)
51. N.M. Cason et al., Phys. Rev. Lett. **36**, 1485 (1976)
52. A.D. Martin, E.N. Ozmutlu, Nucl. Phys. B **158**, 520 (1979)
53. V.A. Polychronakos et al., Phys. Rev. D **19**, 1317 (1979)
54. A. Etkin et al., Phys. Rev. D **25**, 1786 (1982)
55. S. Pislak et al., Phys. Rev. Lett. **87**, 221801 (2001)